Journal of Power Sources 195 (2010) 5543–5549

Contents lists available at ScienceDirect

Journal of Power Sources

journal homepage: www.elsevier.com/locate/jpowsour

Prevention of the water flooding by micronizing the pore structure of gas diffusion layer for polymer electrolyte fuel cell

Yusuke Hiramitsu*, Hitoshi Sato, Michio Hori

Fuel Cell Research Center, Daido University, 10-3 Takiharu-cho, Minami-ku, Nagoya 457-8530, Japan

ARTICLE INFO

Article history:
Received 20 December 2009
Received in revised form 8 March 2010
Accepted 9 March 2010
Available online 16 March 2010

Keywords:
Polymer electrolyte fuel cell
Water management
Flooding
Gas diffusion layer
Microporous layer
Pore structure

ABSTRACT

In polymer electrolyte fuel cells, high humidity must be established to maintain high proton conductivity in the polymer electrolyte. However, the water that is produced electrochemically at the cathode catalyst layer can condense in the cell and cause an obstruction to the diffusion of reaction gas in the gas diffusion layer and the gas channel. This leads to a sudden decrease of the cell voltage. To combat this, strict water management techniques are required, which usually focus on the gas diffusion layer. In this study, the use of specially treated carbon paper as a flood-proof gas diffusion layer under extremely high humidity conditions was investigated experimentally. The results indicated that flooding originates at the interface between the gas diffusion layer and the catalyst layer, and that such flooding could be eliminated by control of the pore size in the gas diffusion layer at this interface.

1. Introduction

Polymer electrolyte fuel cells (PEFCs) are potentially ideal for electricity generation at temperatures between room temperature and about 100 °C in situations requiring a fast cold start or a certain degree of miniaturization. In this regard, they are expected to find practical application in cogeneration systems for homes and in fuel-cell-powered cars. In particular, high performance over a wide temperature range is required for PEFCs to be suitable for automobile use. The ionomer in the catalyst layer (CL) and the polymer electrolyte membrane (PEM) which are used in PEFCs exhibits high proton conductivity in the presence of high water content. Therefore, to achieve high cell performance, it is necessary to humidify the fuel and the oxidant while maintaining a suitable balance between the anode and cathode. Furthermore, to achieve high efficiency, the gas utilization of both the fuel and the oxidant must be increased.

On the other hand, unless the water formed by the reaction at the cathode is completely drained from the CL through the gas diffusion layer (GDL), it blocks the gas channels or the membrane electrode assembly (MEA) and causes a decrease in cell performance, in a phenomenon known as "water jamming". Therefore, to achieve high performance and efficiency, it is necessary to implement strict water management techniques using advanced MEAs [1–3], asymmetric humidification schemes between the electrodes which take into account the water balance in the cell, and gas flow management by optimizing the shape of the gas flow channels and blower [4–7]. Water jamming becomes a particular problem in situations involving a cold start from room temperature, since water condenses easily when the saturated water vapor pressure is low.

The water jamming phenomenon can be roughly classified into "flooding" in the GDL and "plugging" of the gas flow channel [8,9]. For the case of plugging, it was shown that the use of a gas flow channel with a roughened hydrophilic surface caused a considerable reduction in the amount of obstruction to gas diffusion [9].

Attempts to alleviate the problem of flooding in the GDL have been hindered by the fact that the flooding mechanisms are not yet fully understood; this is due in part to the difficulty in directly observing the water between the carbon fibers in the GDL, and also to the complexity involved in simulating the complicated three-dimensional structure of the GDL, which comprises inhomogeneous carbon fibers, a binder and a hydrophobic coating. In recent year, many experimental and theoretical studies have focused on these issues.

Initial studies attempted to determine the relationship between flooding and basic properties of the GDL such as its gas permeability, water-repellency and thickness. In this regard, Williams et al. performed a comparison of several types of GDLs to determine the effects of a number of intrinsic properties, such as limiting current, on oxygen transport, and identified which GDLs were more resistant to flooding [10].

* Corresponding author. Tel.: +81 52 612 6144; fax: +81 52 612 6144.
E-mail addresses: hiramitu@daido-it.ac.jp (Y. Hiramitsu), h-sato@daido-it.ac.jp (H. Sato), hori@daido-it.ac.jp (M. Hori).

0378-7753/$ – see front matter © 2010 Elsevier B.V. All rights reserved.
doi:10.1016/j.jpowsour.2010.03.039

Typically, GDLs are given a water-proofing treatment by polytetrafluoroethylene (PTFE) loading. However, Lin et al. discovered that excessive PTFE loading gave rise to flooding. In addition, they showed that a microporous layer (MPL) promoted back-diffusion of water from the cathode to the anode and reduced the amount of water saturation in the cathode GDL [11].

Ihonen et al. performed power generation and element tests using 6 different types of thick GDLs, with and without MPLs, to investigate the flooding mechanism. They concluded that preventing water jamming in the GDL was more important than attempting to maximize its gas permeability under dry conditions [12]. A detailed study on MPLs performed by Holmstrom et al. indicated that the use of an MPL prevented the cell from water-flooding [1].

In general, it is difficult to produce a homogenous hydrophobic covering on GDL fibers by the use PTFE particles. To combat this problem, Chiu and Wang coated PTFE onto the GDL using a sputtering method, and the resulting fuel cell exhibited a performance comparable to that of a normal sintered GDL with a PTFE dispersion [13].

Other studies were carried out to clarify the mechanisms of flooding in GDLs. Using an interdigitated cell, Yamada et al. observed a loss of pressure in the cell during operation, which indicated that the flooding occurred within the GDL [14]. The present authors have previously examined the dependence of water transport properties on the micropore structure, amount of binder, GDL thickness and water affinity for 21 different kinds of GDL or GDL/MPL structures, and measured the limiting current density under high humidity conditions. The results showed a high correlation between the dehydration pressure, which is an indicator of the ease of drainage, and the limiting current density [15]. Furthermore, the effect of the microstructure at the CL/GDL interface in producing flood-proof GDLs using carbon paper was highlighted [16].

Many studies have focused on the function of the MPL as a water management structure. Atiyeh et al. concluded that higher cell performance could be achieved for cells in which the MPL was under saturated humidity conditions [17]. Antolini et al. demonstrated that higher cell performance was obtained by coating the MPL on the CL side of the GDL than by coating it on the gas channel side. Furthermore, they found that higher PTFE content in the MPL improved cell performance [18], with the optimum value being approximately 30 wt% [19,20].

The properties of the carbon black are also known to have a remarkable influence on the microstructure of the MPL. Using a dry processed MPL developed by our group, Yu et al. compared the effects of Ketjen black and Vulcan black on the cell performance, and found that higher performance was achieved with Ketjen black since it produced more porous electrodes [21,22].

Wang et al. examined the influence of water affinity on the properties of the MPL by using black pearl, acetylene black and a combination of the two. Their results indicated that acetylene black was most suitable as a gas diffusion structure. Furthermore, they found that when acetylene black was mixed with black pearl, the MPL acquired a hydrophilic nature leading to improved drainage characteristics [23].

A large number of simulation studies have been performed to explain these experimental results. Nam and Kaviany investigated gas diffusivity in a water-clogged GDL [24]. Lin et al. performed simulations under two-phase, one-dimensional, steady-state, and isothermal conditions and investigated the relationship between water saturation and overvoltage. They predicted that the influence of flooding in the CL was larger than in the GDL [25].

Meng et al. carried out simulations using a model involving a liquid film coating on a two-dimensional GDL, and discussed the water distribution under the rib and under the channel. The current density under the rib was found to deteriorate under two-phase conditions. In addition, they showed that the water under the rib was removed when the air mass flow increased [26]. Lin and Nguyen reported a similar result, and suggested that water movement along the in-plane direction was important to reduce this flooding [27]. Pasaogullari et al. simulated both water and heat transport, and identified anisotropy between the in-plane and through-plane directions [28,29].

Studies on the structure and composition of the GDL have also been carried out. Wang et al. compared carbon cloth with carbon paper, and found that oxygen diffusion to under the rib was better with carbon cloth because the amount of water saturation was small [30]. Simulations focusing on the microstructure of the GDL were performed by Mukherjee and Wang, who attempted to produce a model which represented the structure of a real GDL. Using this model, they reproduced the pore structure and calculated the capillary pressure. Furthermore, they calculated the effects of compression of the GDL due to cell clamping [31]. Schulz et al. modeled the relationship between GDL morphology and flooding behavior by capillary pressure [32]. Likewise, Inoue et al. analyzed GDL flooding using a networked water transport simulation based on the lattice Boltzmann method. They reproduced an inhomogeneous GDL microstructure and examined the influence of wettability, pore diameter and fiber diameter [33].

Simulations focusing on the role of the MPL in flooding have also been reported [3,34,35]. Pasaogullari et al. examined the effects of MPL thickness, pore volume, and wettability and found that they had a large influence on the degree of water saturation at the CL/MPL interface. This was because increasing the water transport resistance in the cathode led to enhanced back-diffusion of water to the anode, thus reducing both the saturation at the MPL/CL interface and the water flow to the cathode GDL. In addition, the back-diffusion rate was found to increase with increasing MPL hydrophobicity and thickness, and decreasing pore size and porosity [34]. This was considered to be due to capillary pressure in the MPL. It was concluded that a thin, highly hydrophobic MPL had a high potential as a means of preventing flooding in fuel cells [35].

In other words, drainage to the cathode channel is obstructed by an increase of the capillary pressure even if water saturation of the GDL is prevented by a water-repellent treatment. Sinha and Wang came to a similar conclusion for a GDL without an MPL. With regard to flooding of the CL/GDL interface, they proposed a GDL structure with both hydrophilic and hydrophobic regions to carry water and gas, respectively, to achieve a good balance between drainage of water which was clogged at the CL/GDL interface and gas diffusion [36,37].

In recent years, many attempts have been made to visualize the internal workings of fuel cells in order to confirm the results of the experiments and simulations mentioned above [38–42]. Because of the fine microstructure of the GDL, a high spatial resolution imaging technique is required to study it. In addition, high temporal resolution is also needed because the movement of the water is an unsteady process operating over periods from a few seconds to tens of seconds.

Kowal et al. performed quantitative measurements of the in-plane distribution of water in a GDL using neutron radiography. In particular, they focused on the influence of the cloth and paper structures of the GDL. Their results indicated that the reason that carbon paper was more susceptible to flooding than carbon cloth was the presence of large amounts of water under the rib [38].

Using high-resolution X-ray CT methods, Maeda et al. monitored the through-plane water distribution in a GDL by quasi in situ measurements as a function of time, and were able to show the accumulation of water at the CL/GDL interface [41].

In addition, Spernjak et al. visualized the GDL from the gas channel side through a transparent window. Such a basic approach also offers advantages for high temporal resolution [42].

Table 1
GDL specifications. The definition of dehydration pressure was reported in [15].

Manufacturer	Name	Thickness (μm)	Bulk density ($g\,cm^{-3}$)	PTFE content (wt%)	Air permeability ($ml\,cm^{-2}\,h^{-1}\,mm\,Aq^{-1}$)	Water permeability (kPa)	Dehydration pressure (kPa)
Toray	Water-proofed TGP-H-030	111	0.43	11	21,619	3.7	1.2

There is no doubt that large cost reductions must be achieved before practical use can be made of PEFCs. Obviously, the production cost of the GDL must be reduced while maintaining performance. As previously mentioned, for flood-proof GDLs, the use of carbon cloth and a MPL at the CL side each offers performance advantages. Furthermore, it was proposed that the inclusion of both hydrophilic and hydrophobic regions could produce an optimum balance between the water drainage and gas diffusion characteristics of the GDL [37]. The through-holes were made in the GDL in the same purpose [15]. However, these methods lead to higher production costs. The objective of this study is to develop a highly flood-proof GDL structure based on low-cost carbon paper.

The authors have previously proposed that the dehydration pressure is a dominant factor related to flooding from the point of view of water transport through the GDL [15]. However, a weaker correlation was found for a GDL with low dehydration pressure and a second factor was therefore required [16].

In this study, the microstructure of the GDL at the interface with the CL is investigated to determine its relationship to the water transport properties.

2. Experimental

2.1. Microstructure of GDL

2.1.1. GDL preparation

Non-woven carbon paper (TGP-H-030, Toray Industries, Inc., Japan) was used for the GDL. The specifications are shown in Table 1.

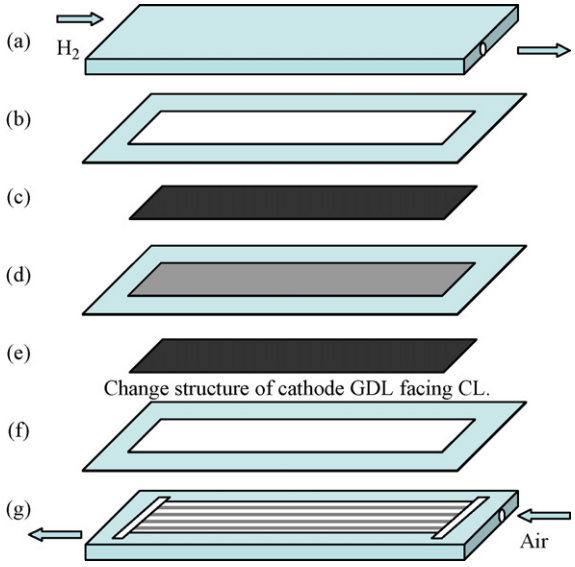

Fig. 1. Detailed view of a single cell prepared for the fuel cell power generation test. (a) Carbon separator for anode, containing 16 channels, 1.0 mm wide and 0.4 mm deep between 1.0-mm-wide ribs. (b) Teflon sheet used as a seal to prevent diffusion of hydrogen from the sides of the anode GDL. (c) Water-proofed GDL. (d) CCM. (e) Water-proofed GDL or water-proofed GDL with water-proofed carbon powder. (f) Teflon sheet used as seal to prevent diffusion of oxygen from the sides of the cathode GDL. (g) Cathode carbon separator, containing 16 channels, 1.0 mm wide and 0.5 mm deep between 1.0-mm-wide ribs. H_2 and air were supplied in a counter-flow configuration, as shown in (a) and (g).

Hydrophobic pretreatment was performed on the GDLs by dipping in a 12 wt% PTFE dispersion (31-JR, DuPont-Mitsui Fluorochemicals Co. Ltd., Japan) and by heating at 350 °C for several minutes in an electric muffle furnace (FUW230PA, Toyo Roshi Kaisha Ltd., Japan). Henceforth, this water-proofed GDL will be referred to as the "WP-GDL".

2.1.2. Micronization of the pore structure at the GDL surface

Micronized GDLs were prepared to evaluate the influence of the contact interface with the CL on the flooding behavior. The following additional water-proofing procedure was carried out on some of the GDLs. Water-proofed carbon powder consisting of PTFE and carbon black was dry-deposited on one side of the water-proofed carbon paper prepared in Section 2.1.1. Carbon black (Vulcan XC-72, particle diameter: 30 nm, specific surface area: $254\,m^2\,g^{-1}$, Cabot Corp., USA) was mixed in a blender with PTFE fine powder (7A-J, particle diameter: 20–60 μm, Du Pont-Mitsui Fluorochemicals Co. Ltd., Japan) in a dry state at a weight ratio of 7:3. In the dry deposition technique, the mixed powder was allowed to absorb through the GDL, and the GDL was then atmospherically sintered in an electric muffle furnace at a temperature of 350 °C to melt the PTFE [21,43]. These GDLs will henceforth be referred to as "Micronized-WP-GDLs".

In comparison to commonly used wet process coating methods, this technique requires only a very small amount of carbon powder. Water-proofed carbon particles can be introduced into the pores of the GDL surface in this manner. Power generation tests were carried out on the basic water-proofed GDL and GDLs with the additional water-proofed carbon powder treatment ($0.05–4.00\,mg\,cm^{-2}$).

2.1.3. Porosimetry

The pore diameter distribution in the carbon fiber and binder was determined by mercury intrusion porosimetry (Poresizer 9320, Micromeritics Instrument Corp., USA).

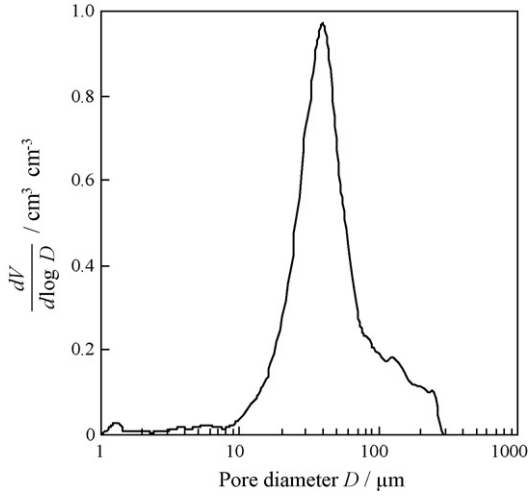

Fig. 2. Pore diameter distribution of water-proofed TGP-H-030 by mercury intrusion porosimetry.

Table 2
The pore parameters of GDL.

Name	PTFE concentration (wt%)	Mean pore diameter, D (μm)	Peak pore diameter, D_{peak} (μm)	Mean porosity ($cm^3\ cm^{-3}$)	Mean specific surface area ($m^2\ cm^{-3}$)
Water-proofed TGP-H-H030	11	24	40	0.54	0.10

2.1.4. Morphology

Scanning electron microscopy (SEM, JSM-6300F, JEOL, Ltd., Japan) was used to evaluate the condition of the binder between the carbon fibers, the adhesion state of the PTFE, the shape of the carbon fibers, and carbon particle adhesion on the GDL.

2.2. Power generation test

The GDL was placed in a fuel cell and power generation was performed to examine the flooding behavior under low and high humidification conditions.

The MEA consisted of a commercially available catalyst-coated membrane (CCM) which was sandwiched between a WP-GDL at the anode side and either a WP-GDL or a Micronized-WP-GDL at the cathode side. The amount of water-proofed carbon powder used in the Micronized-WP-GDLs was 0.05, 0.10, 0.25, 0.50, 1.00, 2.00 and 4.00 mg cm^{-2}. The Pt loading was 0.3 mg cm^{-2} in both the anode and cathode, and the total electrode surface area was $3 \times 15\ cm^2$. The thickness of the PEM was 30 μm. The CCM was used the new one every time to compare the performance between different GDLs.

Fig. 1 shows the structure of the single cells constructed for this investigation.

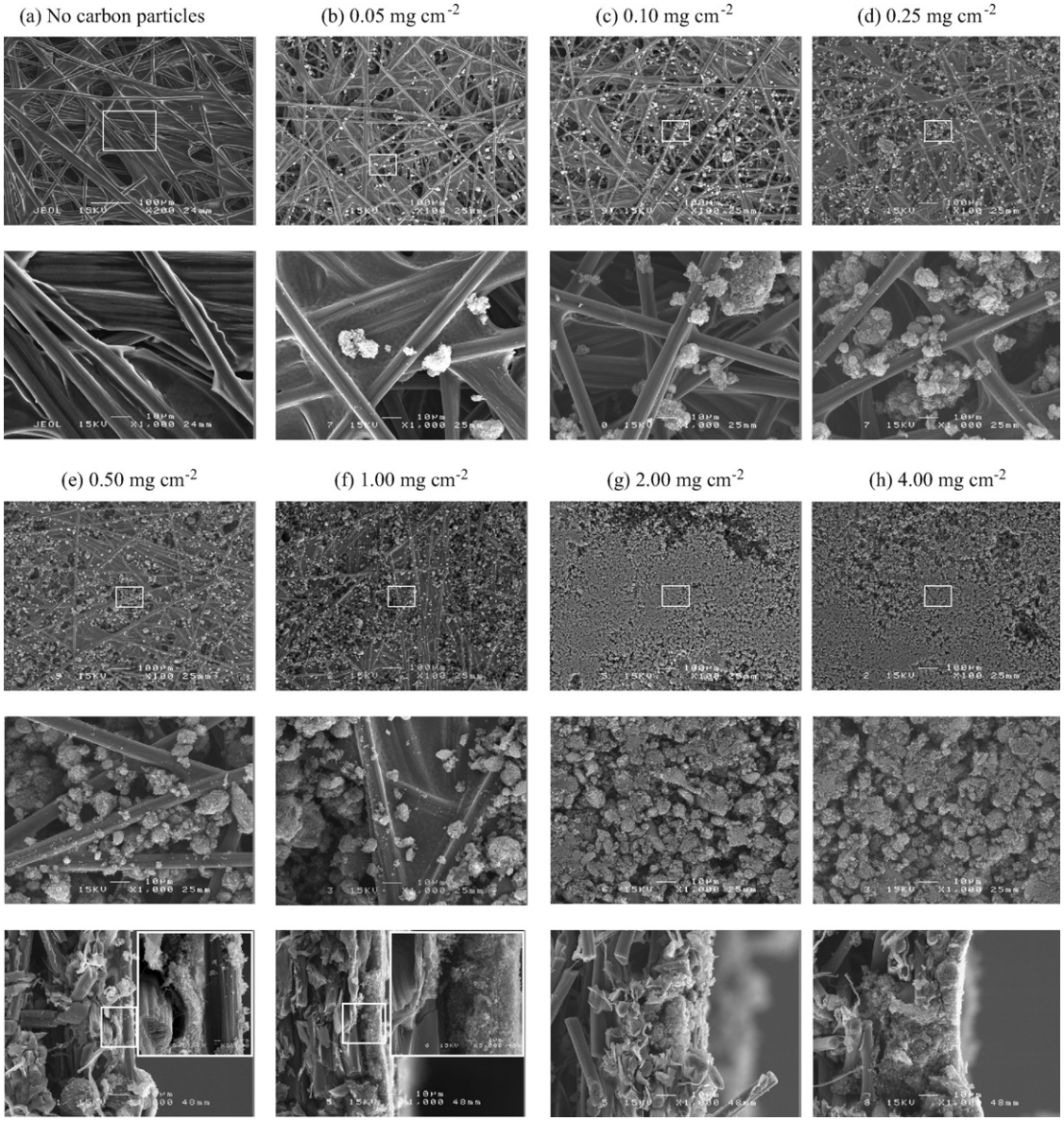

Fig. 3. (a) The SEM images of water-proofed TGP-H-030. The figure below shows the high magnification image in white frame. (b)–(h) The SEM images of water-proofed TGP-H-030 with water-proofed carbon powder as a function of amount of water-proofed carbon powder. The figures just below show the high magnification images in white frame. The bottom of (e–h) shows the cross-sectional images of CL side of GDLs.

A fuel cell test stand (Kojima Instruments Inc., Japan) was used to evaluate the performance of the fuel cell.

The cell was operated at atmospheric pressure. The relative humidities (RHs) of the fuel and oxidant at their respective inlets to the cell were 64%RH at a humidifier temperature of 70 °C and cell temperature of 80 °C, and 100%RH at a humidifier temperature of 75 °C and cell temperature of 75 °C, corresponding to low and high humidification, respectively. The gas utilization of the fuel was 70% for both low and high humidification. The gas utilization of the oxidant was 40% and 70% for low and high humidification, respectively. Before the polarization measurements, the cells were conditioned for 1 day with power generation. The polarization characteristics of the cell were measured by increasing the electric load current (PLZ664WA, Kikusui Electronics Corp., Japan) at a rate of 5 A min^{-1} to a current density of 1.50 A cm^{-2} with constant gas utilization.

3. Results

3.1. Characterization of GDL structure

3.1.1. Pore diameter distribution

The pore diameter distribution of the TGP-H-030 paper measured by mercury intrusion porosimetry is shown in Fig. 2; the approximate pore diameter range is seen to be 10–200 μm. Various pore parameters calculated from this distribution are shown in Table 2.

3.1.2. Morphological characteristics

SEM images of the WP-GDL are shown in Fig. 3(a). Comparatively large pores are seen between the carbon fibers. From the higher magnification image shown in Fig. 3(a), the average diameter of the carbon fibers was determined to be approximately 10 μm. In addition, many large dimples appeared on the surface with diameters of about 100 μm.

SEM images of Micronized-WP-GDLs are shown in Fig. 3(b)–(h). As can be clearly seen in Fig. 3(b)–(f), aggregates of carbon particle adhere to the pores on the surface of carbon paper. Thus, the particles micronize the pores near the surface.

In addition, as can be clearly seen in Fig. 3(g) and (h), when the amount of carbon powder was further increased, a continuous MPL was formed. From the cross-sectional images of CL side of GDLs shown in Fig. 3(g) and (h), the average thicknesses of the MPLs of 2.00 mg cm^{-2} and 4.00 mg cm^{-2} were determined to be approximately 10 μm and 20 μm, respectively.

3.2. Flooding behavior during power generation test

Polarization characteristics were evaluated for low and high humidification conditions to determine the relationship with the GDL surface structure. Fig. 4 shows the cell voltage at a current density of 0.4 A cm^{-2} plotted against the amount of carbon powder. Lower values of cell voltage at 100%RH than at 64%RH indicate the obstruction of gas diffusion due to water condensation. This effect was significant for WP-GDL. On the other hand, the cell voltage increased dramatically following the introduction of just a small amount of water-proofed carbon power (0.10 mg cm^{-2}), which produces the morphology seen in Fig. 3. Furthermore, it can be seen from Fig. 4 that increasing the amount of carbon powder from 0.10 to 2.00 mg cm^{-2} produces a flood-proof effect.

4. Discussion

In this study, flooding behavior during power generation was compared to the observed microstructure of the carbon paper.

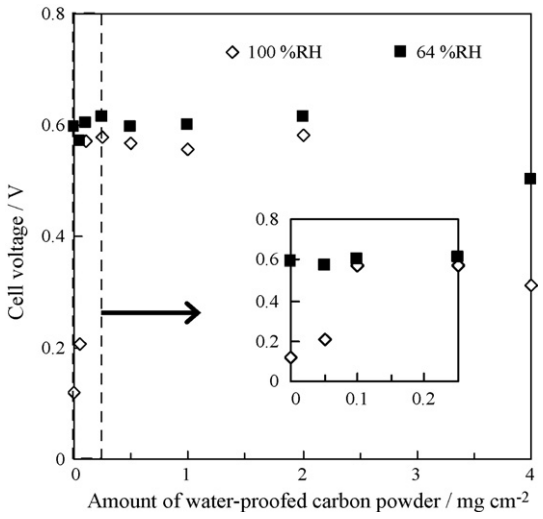

Fig. 4. The relation between the cell voltage at a current density of 0.4 A cm^{-2} and the amount of water-proofed carbon powder. The inset shows an expansion of the region from 0 to 0.25 mg cm^{-2}.

As seen in Fig. 4, for the low humidification single-phase condition, the amount of added carbon powder had no influence on the gas diffusivity up to 2.00 mg cm^{-2}. However, for the 4.00 mg cm^{-2} case, a slight decrease in the cell voltage occurred. This was probably due to a reduction in gas permeability due to the formation of a thick micropore carbon layer, and it is thought that the gas diffusion overvoltage increased [15].

On the other hand, for the high humidification (saturation) condition, a remarkable reduction of the cell voltage was observed for the GDL with no carbon powder addition; this indicates flooding in the cell. However, some improvement occurred even by a carbon powder addition of just 0.05 mg cm^{-2}. Furthermore, at 0.10 mg cm^{-2}, a dramatic increase in the cell voltage was observed, reaching almost to the value for the low humidification case.

This showed that flooding could be prevented by the adherence of a small amount of hydrophobic carbon particles in the GDL at the CL/GDL interface, as seen in Fig. 4. Flooding was controlled in a similar manner to a general MPL for water-proofed carbon addition in the range of 1.00–2.00 mg cm^{-2}. This agrees as a result of previous studies [1,3,11,17,19–23,43,44]. These experimental results show that improvements in cell voltage occur even for a very small amount of GDL pore micronization at the CL/GDL interface, so long as the micronized region does not form a complete layer. This should be distinguished from the normal behavior of MPLs. The concept is shown schematically in Fig. 5. The GDL exhibits a stronger hydrophobicity than the CL which produces water during power generation.

Water transport in a single pore can be expressed by Eq. (1).

$$P = \frac{-4\gamma \cos\theta}{d} \quad (1)$$

P: capillary pressure, γ: interfacial surface tension of water, θ: contact angle; d: pore diameter.

For $\theta > 90°$, P rises with increasing θ, and water transport from the CL surface to the GDL can become difficult when the balance of capillary pressure between the CL and GDL is considered [15,37]. As mentioned above, in such a situation it is believed that the condensed water remains at the CL/GDL interface. If large pores exist at the interface, water droplets will begin to fill these pores until a liquid film covers the CL surface. This film would act as a barrier to gas diffusion, and would be thicker for larger pore diameters. Previous studies have already shown a high degree of water saturation in the GDL at the CL/GDL interface [34,35,37,45]. To prevent flood-

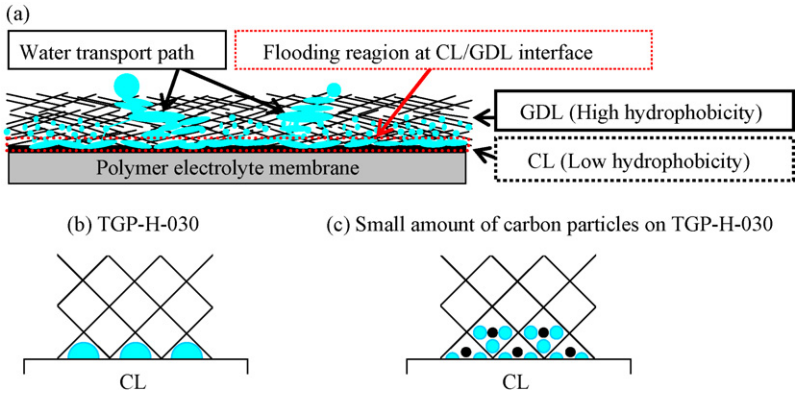

Fig. 5. Conceptual model of GDL flooding based on experimental results. (a) Cathode of the cell. The flooding in water-proofed GDL occurs at the CL/GDL interface due to the mismatch between the hydrophobic GDL and the higher water affinity CL. The water-accumulation model at the CL/GDL interface under two-phase conditions is shown in (b) and (c). (b) Water droplets spreading in large pores. (c) The spread of water droplets is suppressed by the micronized pore structure, and oxygen-diffusion pathways are maintained.

ing, it is believed that it is important to disperse this water into an extensive network of smaller droplets.

The presence of water-proofed carbon particles is likely to prevent the formation of a continuous water layer by producing hydrophobic islands where gas diffusion can still take place.

As shown previously, addition of 4.00 mg cm^{-2} of carbon powder lead to a reduction of the test cell voltage for both humidification conditions. However, under saturation conditions, a larger decrease was observed, which shows the influence of a continuous MPL on flooding.

The use of water-proofed carbon particles can be thought of as producing a microstructure with pore sizes intermediate between those of carbon paper and a MPL. It is believed that optimizing this hybrid pore size should allow the best balance to be achieved between flood-proofing of carbon paper other water transport issues such as dehydration pressure. For this reason, in this study, the relationship between flooding and microstructure was investigated.

Consequently, it is suggested that it should be possible to produce flood-proofed carbon paper with a tailored pore structure, in particular near the CL, by varying the ratio of carbon fiber to binder.

The results of this study suggest a possible method of controlling flooding, which does not lead to the cost increases associated with methods such as the use of carbon cloth, the introduction of hydrophilic regions or the fabrication of macro through-holes. This is important to realize high performance, low-cost fuel cells for practical applications.

In future work, optimization of water management in GDLs will be studied by control of the pore structure.

5. Conclusion

In this study, a mechanism was proposed for flooding in PEFCs, which involved the formation of a continuous water layer at the CL/GDL interface. As a means of preventing such a layer from forming, a novel micropore structure was formed at the interface and its influence on flooding during power generation was evaluated. It was found that the presence of small pores at the interface caused a significant reduction in flooding.

Based on the results, we propose a design guideline for GDLs involving the formation of a water-proofed and micronized pore structure at the surface facing the CL, and simultaneously reducing the thickness of the micronized pore region or the total thickness of the GDL to achieve a balance between the ability to disperse water and the drainage properties.

Acknowledgment

The authors express their special thanks to all those who assisted in the writing of this report. This research was performed under a grant from the Water Management Project from the New Energy and Industrial Technology Development Organization (NEDO) for strategic technical development for the practical realization of PEFCs.

References

[1] N. Holmstrom, J. Ihonen, A. Lundblad, G. Lindbergh, Fuel Cells 7 (2007) 306–313.
[2] X. Ye, C.Y. Wang, Journal of the Electrochemical Society 154 (2007) B676–B682.
[3] A.Z. Weber, J. Newman, Journal of the Electrochemical Society 152 (2005) A677–A688.
[4] Y. Cai, J. Hu, H. Ma, B. Yi, H. Zhang, Electrochimica Acta 51 (2006) 6361–6366.
[5] G.J.M. Janssen, M.L.J. Overvelde, Journal of Power Sources 101 (2001) 117–125.
[6] K.H. Choi, D.H. Peck, C.S. Kim, D.R. Shin, T.H. Lee, Journal of Power Sources 86 (2000) 197–201.
[7] Q. Yan, H. Toghiani, J. Wu, Journal of Power Sources 158 (2006) 316–325.
[8] H. Masuda, K. Ito, T. Oshima, K. Sasaki, Journal of Power Sources 177 (2008) 303–313.
[9] M. Shoyama, T. Tomimura, S. Mizutani, ECS Transactions 17 (2009) 461–464.
[10] M.V. Williams, E. Begg, L. Bonville, H.R. Kunz, J.M. Fenton, Journal of the Electrochemical Society 151 (2004) A1173–A1180.
[11] G. Lin, T.V. Nguyen, Journal of the Electrochemical Society 152 (2005) A1942–A1948.
[12] J. Ihonen, M. Mikkola, G. Lindbergh, Journal of the Electrochemical Society 151 (2004) A1152–A1161.
[13] K.F. Chiu, K.W. Wang, Surface & Coatings Technology 202 (2007) 1231–1235.
[14] H. Yamada, T. Hatanaka, H. Murata, Y. Morimoto, Journal of the Electrochemical Society 153 (2006) A1748–A1754.
[15] Y. Hiramitsu, K. Hirose, K. Kobayashi, M. Hori, Transactions of Materials Research Society of Japan 33 (2008) 1113–1117.
[16] Y. Hiramitsu, K. Okada, K. Kobayashi, M. Hori, in: Fiber Preprints, vol. 63, A1 The Society of Fiber Science and Technology, Japan, 2008, p. 192.
[17] H.K. Atiyeh, K. Karan, B. Peppley, A. Phoenix, E. Halliop, J. Pharoah, Journal of Power Sources 170 (2007) 111–121.
[18] E. Antolini, R.R. Passos, E.A. Ticianelli, Journal of Applied Electrochemistry 32 (2002) 383–388.
[19] J.M. Song, S.Y. Cha, W.M. Lee, Journal of Power Sources 94 (2001) 78–84.
[20] Z. Qi, A. Kaufman, Journal of Power Sources 109 (2002) 38–46.
[21] J. Yu, Y. Yoshikawa, T. Matsuura, M.N. Islam, M. Hori, Electrochemical and Solid-State Letters 8 (2005) A152–A155.
[22] J. Yu, M.N. Islam, T. Matsuura, M. Tamano, Y. Hayashi, M. Hori, Electrochemical and Solid-State Letters 8 (2005) A320–A323.
[23] X.L. Wang, H.M. Zhang, J.L. Zhang, H.F. Xu, Z.Q. Tian, J. Chen, H.X. Zhong, Y.M. Liang, B.L. Yi, Electrochimica Acta 51 (2006) 4909–4915.
[24] J.H. Nam, M. Kaviany, International Journal of Heat and Mass Transfer 46 (2003) 4595–4611.
[25] G. Lin, W. He, T.V. Nguyen, Journal of the Electrochemical Society 151 (2004) A1999–A2006.
[26] H. Meng, C.Y. Wang, Journal of the Electrochemical Society 152 (2005) A1733–A1741.
[27] G. Lin, T.V. Nguyen, Journal of the Electrochemical Society 153 (2006) A372–A382.

[28] U. Pasaogullari, C.Y. Wang, Journal of the Electrochemical Society 151 (2004) A399–A406.
[29] U. Pasaogullari, P.P. Mukherjee, C.Y. Wang, K.S. Chen, Journal of the Electrochemical Society 154 (2007) B823–B834.
[30] Y. Wang, C.Y. Wang, K.S. Chen, Electrochimica Acta 52 (2007) 3965–3975.
[31] P.P. Mukherjee, C.Y. Wang, Journal of the Electrochemical Society 154 (2007) B419–B426.
[32] V.P. Schulz, J. Becker, A. Wiegmann, P.P. Mukherjee, C.Y. Wang, Journal of the Electrochemical Society 154 (2007) B419–B426.
[33] G. Inoue, T. Yoshimoto, Y. Matsukuma, M. Minemoto, Journal of Power Sources 175 (2008) 145–158.
[34] U. Pasaogullari, C.Y. Wang, K.S. Chen, Journal of the Electrochemical Society 152 (2005) A1574–A1582.
[35] U. Pasaogullari, C.Y. Wang, Electrochimica Acta 49 (2004) 4359–4369.
[36] P.K. Sinha, C.Y. Wang, Electrochimica Acta 52 (2007) 7936–7945.
[37] P.K. Sinha, C.Y. Wang, Chemical Engineering Science 63 (2008) 1081–1091.
[38] J.J. Kowal, A. Turhan, K. Heller, J. Brenizer, M.M. Mench, Journal of the Electrochemical Society 153 (2006) A1971–A1978.
[39] C. Hartnig, I. Manke, N. Kardjilov, A. Hilger, M. Grunerbel, J. Kaczerowski, J. Banhart, W. Lehnert, Journal of Power Sources 176 (2008) 452–459.
[40] P.K. Sinha, P.P. Mukherjee, C.Y. Wang, Journal of Materials Chemistry 17 (2007) 3089–3103.
[41] M. Maeda, Y. Isogai, M. Shiozawa, G. Tejima, H. Hamada, Denso Technical Review 13 (2008) 37–43.
[42] D. Spernjak, A.K. Prasad, S.G. Advani, Journal of Power Sources 170 (2007) 334–344.
[43] J. Chen, T. Matsuura, M. Hori, Journal of Power Sources 131 (2004) 155–161.
[44] G. Velayutham, J. Kaushik, N. Rajalakshmi, K.S. Dhathathreyan, Fuel Cells 7 (2007) 314–318.
[45] U. Pasaogullari, C.Y. Wang, K.S. Chen, Proceedings of IMECE04 (2004) 1–9.